Dose-Response:
An International Journal
January-March 2020:1-10

DOI: 10.1177/1559325820907741
journals.sagepub.com/home/dos
SAGE

Effects Induced In Vivo by Exposure to Magnetic Signals Derived From a Healing Technique

Sarah Beseme[1,2], Loren Fast[3], William Bengston[4], Michael Turner[5], Dean Radin[6], and John McMichael[1,2]

Abstract

Energy healing is a therapy said to manipulate and balance the flow of "energies" in the body. One such technique, the Bengston Healing Method (BHM), has shown some success in healing malignant tumors in animals and humans, but the mechanism of action and factors influencing therapeutic success of this method is poorly understood. In this study, we tested in vivo the antitumor potential of magnetic signals recorded during BHM healing. Balb/c mice engrafted with 4T1 breast cancer cells were exposed to this recording for 4 h/d on a weekly or daily basis for 28 days; control mice were not exposed at all. Tumors showed a trend to grow slower in the treatment versus control group during the fourth week of treatment. Elevated leukocyte counts, associated with an increase in blood levels of granulocyte–macrophage colony stimulating factor and interleukin-6, were observed in tumor-bearing mice exposed to the BHM recording but not in healthy animals exposed to the recording. This suggests that exposure to a recording of BHM may induce a biological response in tumor-bearing mice, but limited effects on tumor growth when observed within the predefined end point of 28 days. Studies involving longer end points are recommended to observe the progression of tumor growth.

Keywords

energy medicine, audio, integrative medicine, breast cancer, healing, magnetic signals

Introduction

Increasingly, patients are considering complementary and alternative approaches for treatment of serious diseases, such as cancer. In response, academic cancer institutes are proposing integrative medicine therapies in addition to traditional treatments.[1] Among those, the category of "healing touch" (HT) has been qualified as a mind–body intervention by the US National Center for Complementary and Integrative Health. This type of intervention is a form of the so-called energy healing, an intentional technique said to manipulate and balance the "energies" of the body; it has been reported to be beneficial on a wide variety of conditions, usually in combination with more traditional therapies.[2]

There are many variations in the practice of energy healing. One common feature is that the healer seems to promote self-healing in the patient, rather than literally send energy to the patient; another is that the healer and patient do not need to be near each other. In other words, the terms "energy healing" and "healing touch" may both be misnomers in that these techniques do not appear to involve a transfer of energy, at least not as energy is commonly defined within current physics, and HT does not necessarily require close proximity.

Because of the heterogeneity in energy healing practices, as well as the variability in responses to treatment, the underlying mechanisms are poorly understood, and their therapeutic potential is yet to be reliably demonstrated. Reviews of clinical

[1] Beech Tree Labs, Inc, Providence, RI, USA
[2] The Institute for Therapeutic Discovery, Delanson, NY, USA
[3] Division of Hematology/Oncology, Rhode Island Hospital, RI, USA
[4] St Joseph's College, Port Jefferson, NY, USA
[5] Institute of Electrical and Electronic Engineer, MDT Consulting, Huntsville, AI, USA
[6] Institute of Noetic Sciences, Petaluma, CA, USA

Received 22 July 2019; received revised 8 January 2020; accepted 16 January 2020

Corresponding Author:
Sarah Beseme, Beech Tree Labs, Inc, 1 Virginia Avenue Providence, RI 02905, USA.
Email: sarah.beseme@beechtreelabs.com

trials testing energy healing for various diseases suggest that therapeutic potential that may be more readily demonstrated with improved study designs, for example, focusing on targeted outcomes or clarifying methods used for the intervention, among others.[3]

We have developed a method to record magnetic and electromagnetic signals associated with energy healing, then play back that recording to test if it mimics the effect of a live healer. The energy healing technique we have focused on is the Bengston Healing Method (BHM), a technique developed in the early 1970s.[4,5] Anecdotal reports and laboratory tests by BHM practitioners suggest that it is effective in treating cancer in human and animals. We recently investigated effects of exposing cancer cells in vitro to a recording of the BHM technique.[6] Results showed that transcription of genes involved in cancer and immunity pathways were affected by the recording, even though the relative strength appeared to be less than the direct hands-on method. Based on those results, we conducted an in vivo pilot investigation of the effect of the same recording on tumor growth and disease outcome in a syngeneic breast cancer mouse model.

Methods

Cell Line

The murine mammary tumor cells 4T1 (ATCC, Manassas, Virginia) were cultured in RPMI (Gibco, Thermo Fisher, Waltham, Massachusetts) supplemented with 10% fetal bovine serum (FBS, Gibco) and maintained at 37°C in a humidified atmosphere with 5% CO_2. Cells were passaged by trypsinization twice a week.

Animals

All animal experiments were approved by the Institutional Animal Care and Use Committee of Lifespan and were conducted per approved protocol. On day 1 of the study, 8-week-old female Balb/c mice were subcutaneously injected with 100 000 4T1 cells in the flank above the leg and the animals were randomized in 3 treatment groups: control (no exposure, N = 5), weekly exposure (N = 10), and daily exposure (N = 10). The procedure for exposure to BHM recording is detailed below.

Blood samples were collected once a week for all mice, including before initiation of treatment.

All animals but 3 in each group were euthanized on day 21 as they reached a criterion for euthanasia (ulceration or tumor size > 2 cm^3). The 9 remaining mice were allowed to develop ulcers per protocol and were euthanized on day 28 as the calculated tumor volume reached 2 cm^3. In addition, 15 mice (5 for control, 5 for daily exposure, and 5 for weekly exposure) were subjected to the same treatment regimen, including blood collection, without injection of cancer cells.

Recording of BHM

To record the BHM healing process, 3 BHM practitioners located inside a solid steel, double-walled, electromagnetically shielded chamber (ETS-Lindgren, Cedar Park, Texas, Series 81 Solid Cell) directed their healing intentions for 5 minutes toward samples of organic cotton. As the treatment of cotton took place, 4 types of sensors in the shielded chamber recorded ambient magnetic and electromagnetic signals. They included (1) eleven 3-axis magnetoresistive sensors (Honeywell model HMC2003, sensitivity 50 microGauss from DC-1 kHz), (2) 2 "mini-Whip" active antennas (Roelof Bakker, http://dl1dbc.net/SAQ/miniwhip.html) recording electromagnetic fields above 10 kHz, (3) a geomagnetometer (Integrity Design, Essex Jt, Vermont, model IDR-321, sensitivity 1 milliGauss, DC-500 Hz), and (4) 2 custom-fabricated so-called "Caduceus" coils, designed to cancel out transverse electromagnetic waves. Each of these 38 analog signals was digitized by a 24-bit analog-to-digital converter at 44.1 kHz (model Motu 24ai; Motu, Cambridge, Massachusetts). Custom PC software converted and saved the incoming sensor signals into the .wav audio format, which could be played back later as an audio file. The present studies focused on the recording of the 33 magnetic signals.

Treatment

The treatment consisted of 4 hours of exposure to the recording. The audio system playing the recording was placed on a shelf above the mice cages with the speakers pointing down toward the cages. This system was described in more detail in a previous publication.[6] During the period of exposure, the recording was repeatedly played on a loop by a computer connected to an amplifier with passive speakers. The volume of the computer and the player, software, as well as the amplifier was set at 50%. The amplifier was under the control of a timer, which allowed the sound to be played continuously for 4 h/d. Following engraftment, mice in the daily exposure group were housed in the dedicated room. Mice in the weekly exposure group were brought once a week into the room, while mice in the control group were housed in a distant general housing room. Healthy animals were subjected to the same treatment as the tumor-bearing mice.

Sample Collection and Storage

Blood was collected on day 0 (before injection with 4T1), and on days 7, 14, 21, and 28 after injection by cheek bleed and by cardiac puncture at euthanasia. For cheek bleeds, samples from 2 to 3 mice were pooled in the same tube to increase the working volume. Plasma was isolated by centrifugation after a complete cell blood count was performed and stored at −20°C for further cytokine-level measurements. Tumors were excised at euthanasia and a portion was snap-frozen and stored at −80°C for further real-time polymerase chain reaction (RT-PCR) analysis. Another portion was stored in 10% neutral-buffered formalin (Richard Allan Scientific, San Diego,

California) for immunohistochemistry staining. Spleens were excised and splenocytes were obtained by dissociating a section of the spleen in phosphate buffer saline (PBS). After one wash, the cells were resuspended in RPMI 1640 (Gibco) containing 4% FBS (Atlanta Biological, Flowery Branch, Georgia), 2 mg/mL glucose (Sigma Aldrich, St. Louis, Missouri), 2 mM glutamine (Gibco), penicillin/streptomycin (Gibco), and 10 μM 2-mercaptoethanol (Sigma Aldrich). The splenocytes were directly used for immunophenotyping or were cultured at a concentration of 1.5×10^6 cells/mL overnight at 37°C and the supernatant was collected at 24 hours and stored at −20°C for further measurement of cytokines.

Assessment of Tumor Growth and Health of the Animals

The weight of each mouse was measured 3 times a week. To measure tumor growth, 2 perpendicular measurements were taken with electronic calipers (GlowGeek, China) every 2 to 3 days when the tumors started to appear. Tumor volume (Tv) was calculated using the following formula: $Tv = L \times W \times W/2$, where L (length) is the short measurement and W (width) is the longest measurement. Every week, complete cell blood count was evaluated using the HemaTrue Veterinary Hematology Analyzer (Heska, Loveland, Colorado), according to the manufacturer's instructions.

Cytokine Panels

Cytokines levels in plasma and splenocytes supernatants were measured using the Millliplex MAP mouse cytokine/chemokine magnetic kit (Millipore, Burlington, Massachusetts), according to the manufacturer' instructions. Briefly, samples were incubated overnight with a mix of 25 microspheres coated with capture antibodies. After washes, the biotinylated detection antibody was added for 1 hour, followed by incubation streptavidin–phycoerythrin conjugate. The signal of individual microspheres was analyzed using the Luminex 200 with Xponent software (Biorad, Hercules, California), according to the manufacturer's instructions. The following cytokines were included in the kit: granulocyte-colony stimulating factor (GCSF), granulocyte–macrophage colony stimulating factor (GM-CSF), interferon-γ, interleukin (IL)1A and IL1B, IL2, IL4, IL5, IL6, IL7, IL9, IL10, IL12(p40), IL12(p70), IL13, IL15, and IL17, IP10, MKC, MCP-1, MIP-1A and MIP-1B, MIP-2, RANTES, and tumor necrosis factor-α.

Quantitative Real-Time Polymerase Chain Reaction

Frozen tumor samples were thawed in RNALater ICE (Thermo Fisher) overnight and homogenized using a mechanical homogenizer (Polytron, Kinematica, New York) in TRIzol (Thermo Fisher). Total messenger RNA was extracted following the manufacturer's instructions. Complementary DNA (cDNA) was synthetized using RT2 First-Strand Kit (Qiagen, Germantown, Maryland) from 250 ng of RNA and expression of genes was analyzed using RT2 pPCR Primer Assay (Qiagen), according to the manufacturer's instructions. One microliter of cDNA was used in the PCR reactions. Results were analyzed using the ΔΔCt method.

Immunophenotypic Analysis

Cells used for immunophenotyping studies were either splenocytes or leukocytes obtained from blood. When mice were euthanized, blood was collected via cardiac puncture using a syringe that had been rinsed with 10% potassium ethylenediaminetetraacetic acid. The blood was placed in a 1 mL Wintrobe tube (Fisher Scientific, Hampton, New Hampshire) and centrifuged at 2000 rpm for 10 minutes. The plasma was removed and stored at −20°C for future analysis. The buffy coat was collected and placed in 2 mL of red blood cell solution for 10 minutes at room temperature. Then 10 mL of PBS was added and the tubes were centrifuged at 1500 rpm for 5 minutes. The cells present in the pellet or splenocytes were incubated with a panel of labeled monoclonal antibodies: anti-CD3 PE-Cy7, CD4 BV605, CD8 APC-H7, natural killer (NK)1.1 APC, and CD19 V450 (BD Biosciences, San Jose, California) in staining buffer on ice in the dark for 20 minutes. Cells were then washed in the staining buffer and resuspended in staining buffer and analyzed on an LSRII flow cytometer (BD Biosciences). Isotype controls were used for each experiment. Results were analyzed using FlowJo version 10 software (FlowJo, LLC, Ashland, Oregon).

Statistical Analyses

Student t tests were used to determine P values between control group (nonexposed) and experimental groups (exposed); P values less than 0.05 were considered statistically significant.

For PCR, Ct values were analyzed using the online tool Data resources Center (Qiagen.com), and fold-changes ($2^{-\Delta\Delta Ct}$) were determined as the normalized gene expression ($2^{-\Delta Ct}$) in the experimental sample divided by the normalized gene expression ($2^{-\Delta Ct}$) in the control sample; P values were calculated based on a Student t test of the replicate $2^{-\Delta Ct}$ values for each gene in the control group and treatment groups.

Results

Effect of BHM Recording on Tumor Growth and General Health

Tumors started to appear on day 9 postengraftment in all groups. On day 16, ulceration appeared on the tumors and the first 3 ulcerated mice in each treatment group were separated from their littermates and transferred to a new cage (1 new cage per group). All of the other mice were euthanized on day 21 because they reached a criterion for euthanasia (ulceration or tumor size > 2 cm^3). The 9 remaining mice were euthanized on day 28, as the ulcers or tumors had reached the maximum size (5 mm and 2 cm^3, respectively). Control mice not injected with tumor cells but subjected to the same treatment regimen were euthanized on day 28. Despite the size of the tumors and for some mice the dragging of the injected leg, tumor-bearing mice

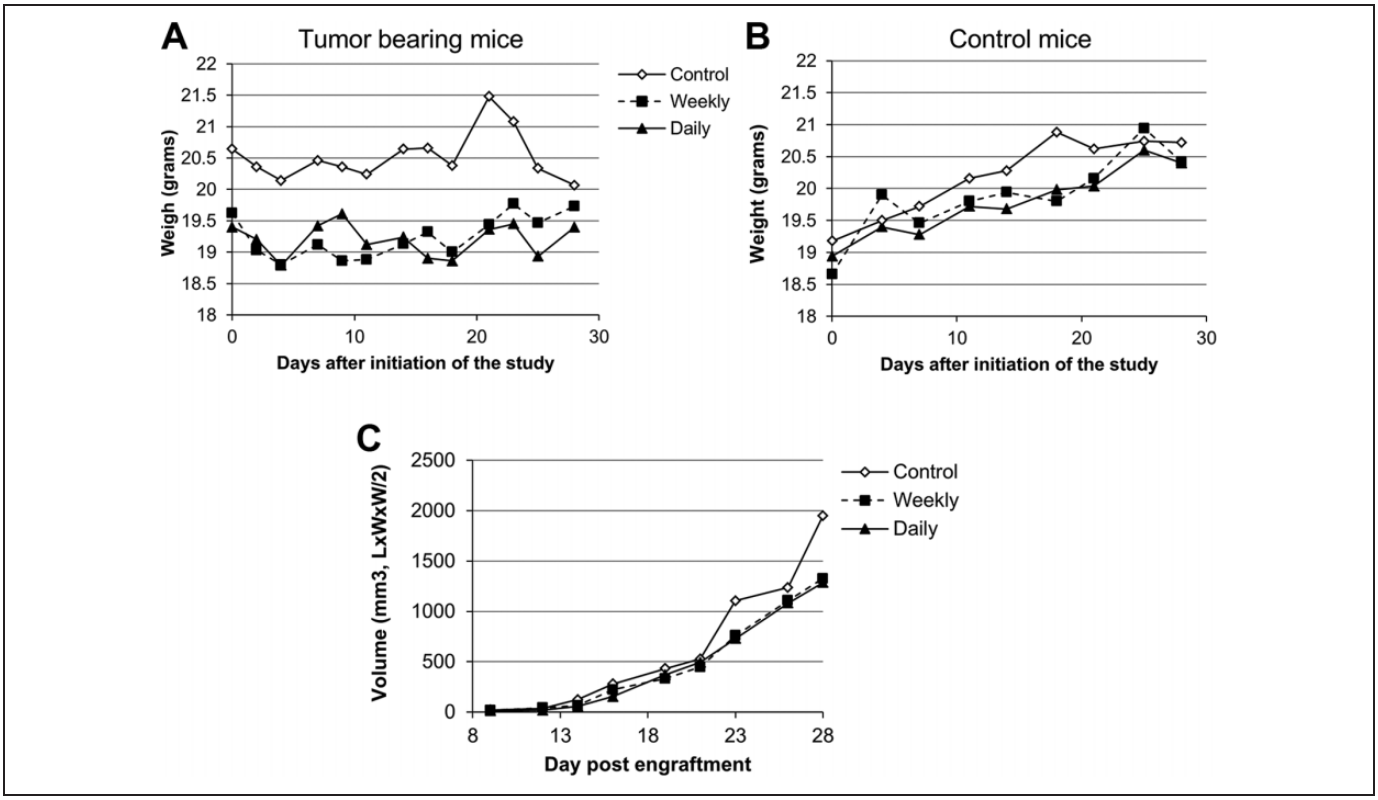

Figure 1. Weight and tumor size throughout the study. A and B, Weight of mice. The weight of each mouse was measured 3 times a week. Graphs show the average weight in each group (control, weekly, and daily exposure) throughout the study for tumor-bearing mice (A) and tumor-free control mice (B). C, Tumor size. Two perpendicular measurements were taken with electronic calipers every 2 to 3 days when the tumors started to appear. Tumor volume (Tv) was calculated using the following formula: $Tv = L \times W \times W/2$, where L (length) is the short measurement and W (width) is the longest measurement. Data represent the average of all mice in each group. For day 21 and beyond, data represent the average of 3 mice per group remaining in the study.

looked healthy and were grooming, eating, and drinking similarly to the noninjected controls. No loss or gain of weight was observed (Figure 1A and B). As measured by calipers, the size of tumors in the control group tended to be greater than in both treatment groups at later time points, corresponding to the 9 remaining mice (Figure 1C). However, the average weight of tumor tissue excised after euthanasia did not vary between the groups (not shown), presumably because some samples contained muscle tissue in tumors embedded in the leg. Hematoxylin/eosin staining of tumor sections revealed a classic aggressive cancer phenotype with mitotic areas and necrotic areas due to lack of blood supply (Supplemental data 1). There was no difference between the treatment and control groups.

Exposure to the Recording Induced an Increase in Myeloid Cells

A complete blood count (CBC) was performed on samples collected every week and at euthanasia. All parameters were normal throughout the study, except for the leukocyte count in tumor-bearing mice. We observed an increase in leukocytes in all groups over the time, as it has been described in this model.[7] We found that this increase was more pronounced in the daily treatment group than in the control group (Figure 2A). The weekly group showed an intermediate count, suggesting a possible dose response to the treatment. No change in the leukocyte count was observed in tumor-free mice exposed to the recording. The difference between the control and the treatment groups was attributed to an increase in myeloid cells, specifically granulocytes (Figure 2B). Blood samples collected at euthanasia confirmed this trend. There were more samples for which the leukocyte count exceeded the limit of detection of the analyzer (100 000 cells/μL) in the daily treatment group than in the weekly treatment group or in the control group (Figure 3A). The leukocyte count was significantly increased in the daily exposure group than in the 2 other groups (Figure 3B). These results were associated with an increase in the size of the spleen. Enlargement of the spleen is common in murine models of cancer and has been described previously for the 4T1/Balb/c model.[8] In tumor-bearing mice exposed to the recording, the weight of the spleen was increased 8-fold as compared to healthy mice, while there was a 5-fold increase in the control group (Table 1).

Effect of the Recording on Lymphocyte Populations

The complete blood count results did not show a difference of the total lymphocyte count between the groups. We

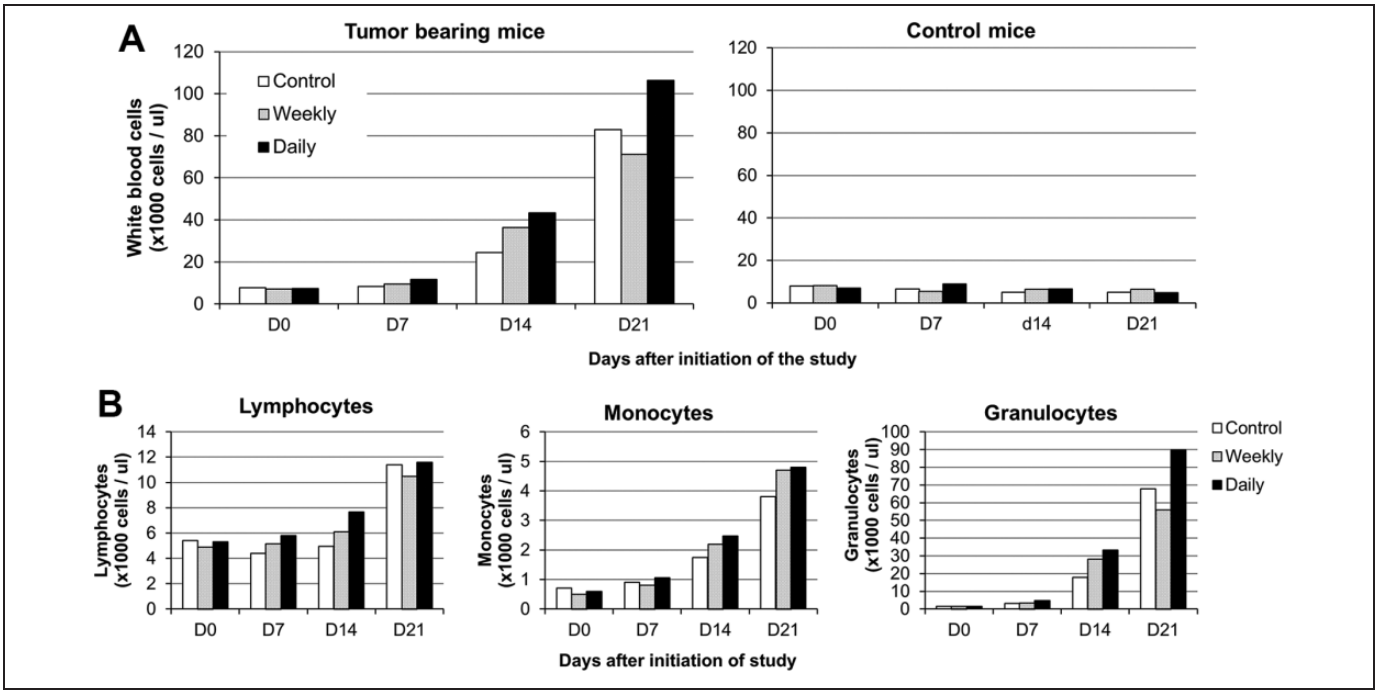

Figure 2. Increase in leukocytes throughout the study. A, Leukocyte count throughout the study. In tumor-bearing mice (left panel), leukocytes (white blood cells) started to increase slightly in the daily treatment group on day 7. All groups show an increase in leukocytes at day 14 and day 21, more pronounced for the daily treatment group. In control animals, leukocytes remained stable at low level. B, Leukocyte subtypes count in tumor-bearing mice. All 3 types of leukocytes (lymphocytes, monocytes, and granulocytes) were increased, but granulocyte was the cell type that contributed for most of the increase in leukocytes. Bars represent the average of all mice in each group. On day 21, the blood of the 3 mice in each group was pooled into one sample.

investigated the cellular composition of the lymphocyte population by flow cytometry to identify a potential effect of the recording in tumor-bearing mice. The proportion of T cells, B cells, and NK cells was examined using the blood samples collected throughout the study. Results showed an increase in B cells in all groups in the course of the study, with a peak at day 15 (Figure 4A), no change in CD4+ and CD8+ T cells (Figure 4B and C). Interestingly, NK and NKT cells were increased in the control group at day 15 and 21, suggesting a possible anticancer response (Figure 4D and E). In the group of mice treated daily, this increase was lower but appeared earlier.

Cytokine Profile

We then investigated the cytokine profile of blood samples and splenocyte supernatants collected at euthanasia in the tumor-bearing mice, using a panel of 25 cytokines. Table 2 shows the fold-change (upper value) and *P* value (*t* test, bottom value) of cytokine levels in the weekly and daily treated group as compared to the control group. The largest changes were observed with GM-CSF and IL7: 17- and 4.9-fold increase at D14 and D21, respectively. Expression of GM-CSF was measured by RT-PCR in the tumors (Figure 5A). Results showed a modest but significant increase in the expression level in the daily group, and an intermediate level in the weekly group, which was a similar trend observed with the cytokine profile and also with the increase in granulocytes in the blood.

Interleukin-6 produced by splenocytes increased in the daily treatment group at day 21 (Table 2). However, it was consistently decreased in the blood at all time points with the daily treatment. Interleukin-6 promotes expression of antiapoptotic genes such as B-cell lymphoma 2 (*BCL2*) or genes that participate in metastasis formation, such as matrix metalloproteinase 9 (*MMP9*).[9,10] We investigated the IL6-mediated signaling in the tumors by qRT-PCR and found that IL6 showed a trend to increase in the tumors in both the weekly and daily groups (Figure 5B), though the increase was not statistically significant. BCL2 was significantly increased in the daily group (Figure 5C) and MMP9 was significantly increased in both groups, with a 2.94-fold increase in the weekly group (Figure 5D and Table 3).

Discussion

It was hypothesized that healing potential could be "captured" in a recording, which could in turn reproduce the effect of healing with intent. To test this hypothesis, we exposed tumor-bearing mice to a recording that previously suggested the induction of biologic changes in vitro.[6] In the present study, no significant effects of the recording on tumor growth were observed up to 21 days, but at the predefined end of the study, tumors in the treated group tended to be smaller than in the control group.

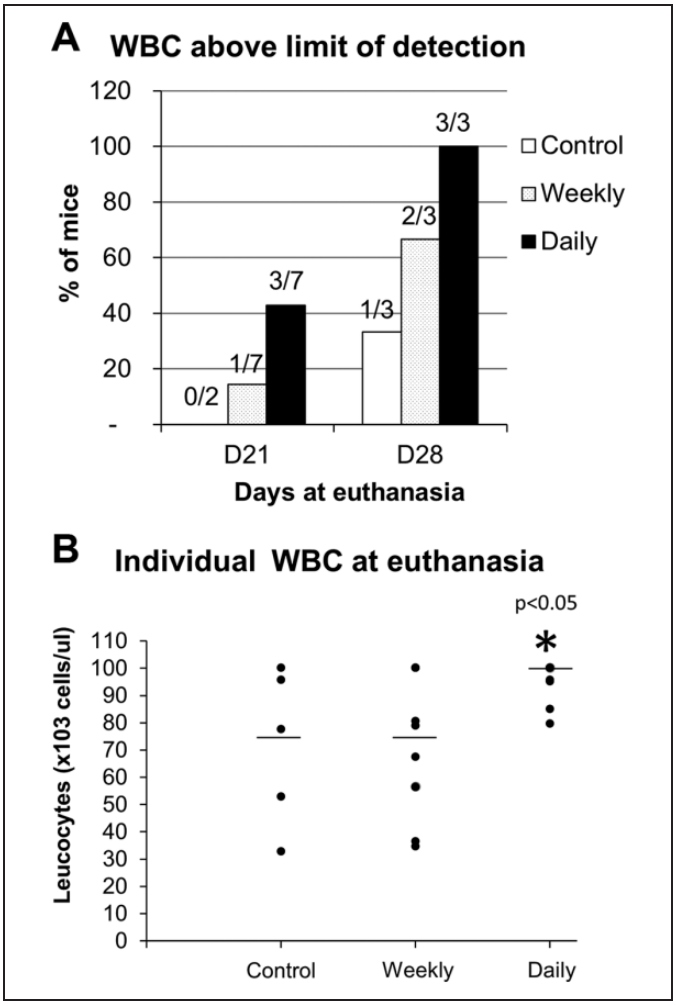

Figure 3. Increase in leukocytes above the limit of detection at euthanasia. A, Percentage of samples for which the white blood cell (WBC) count was >100 000 cells/μL, which is the limit of detection of the machine used for the complete blood count, at euthanasia. All mice from the daily treatment group euthanized at day 28 had a higher WBC count. B, Leukocyte count in each sample at euthanasia. Each dot represents one animal. Samples above the limit of detection were artificially set up to 100 000 cells. The average leukocyte count, represented by the horizontal bars, was significantly higher in the daily group than in the control or weekly group. ($P < .05$, unpaired, 2-tailed t test).

Table 1. Enlargement of the Spleen.[a]

Treatment	Spleen Weight (g)		Ratio Tumor/Control
	Control, n = 5	Tumor Bearing, n = 3	
Control	0.09 (0.01)	0.51 (0.17)	5.67
Weekly	0.06 (0.01)	0.48 (0.16)	8.00
Daily	0.08 (0.02)	0.62 (0.13)	7.56

[a]Spleens were weighted at day 28 for the tumor-free mice (5 animals per group) and tumor-bearing mice (3 animals per groups). The first 2 columns display the average weight and standard deviation in parenthesis. The last column displays the ratio of the average weight in each group.

In an independent study reminiscent of this observation, researchers reported a moderate effect of HT on tumor progression in the 4T1/Balb/c model.[11] Those investigators exposed mice injected with tumor cells to HT in sessions of 10 minutes every day or every other day over a period of 10 days. Although no statistically significant difference was reported in that study, the tumor in control mice (ie, not exposed to HT and housed in a separate room) tended to be bigger than those in the mice exposed to HT. The authors of that study argued that refinements of dose, frequency, and duration might improve the quality of results.

The most interesting result in our experiment was an increase in myeloid cells in the blood of tumor-bearing mice exposed to the recording. This was associated with an increase in GM-CSF in the tumor environment as well as in the blood. The role of GM-CSF in breast cancer is dual: On one hand, it can lead to the generation of myeloid-derived suppressor cells (MDSCs) that are associated with tumor progression, as their role is immunosuppressive.[12,13] On the other hand, GM-CSF in the microenvironment of the tumor has been shown to decrease tumor progression by recruiting antigen-presenting cells.[14] Other immune cells can be activated in response to GM-CSF, including T cells, granulocytes, macrophages, and NK cells.[15] Our results suggested that the increase in GM-CSF may not be associated with MDSCs. Granulocyte-colony stimulating factor, which also participates in granulocyte differentiation and not in MDSCs proliferation, was elevated in the spleen of daily treated mice at day 28. In addition, immunophenotypic analysis revealed no changes in the number of CD11b+Ly6-G+ MDSCs cells between groups at day 28 in both the spleen and the blood (data not shown). Immunofluorescence staining of tumor sections revealed the presence of $CD11b^{+}Gr\text{-}1^{+}$ MDSC in necrotic areas within the tumors (Supplemental data 1), as described in other cancers.[16] There were no apparent difference between the groups.

However, we did observe an increased production of IL6 by the splenocytes of mice exposed to the recording. Interleukin-6 is generally associated with tumor progression in breast cancer, as it promotes proliferation of MDSCs and transcription of antiapoptotic and promigratory genes, such as *BCL2* and *MMP9*. Consistent with the increase in IL6, we found that expression of these 2 genes was increased in the tumor of treated mice as compared to the control group. The qRT-PCR results were unexpected as they suggest a promotion of the tumor phenotype. In addition, expression of IL1 was upregulated in the spleen with the daily treatment, and levels of IL1β were higher in the daily group than the control in the blood samples throughout the study. This result was surprising because in our previous study, we found that IL1β expression was downregulated in breast cancer cell lines when exposed to either the recording or to the hands-on delivery of BHM.[6] We did not find any difference in the tumor expression of IL1β in the present study by qRT-PCR. Interleukin-1β is mostly associated with metastasis in breast cancer, but we did not see clinical or anatomical signs of metastasis in our study.

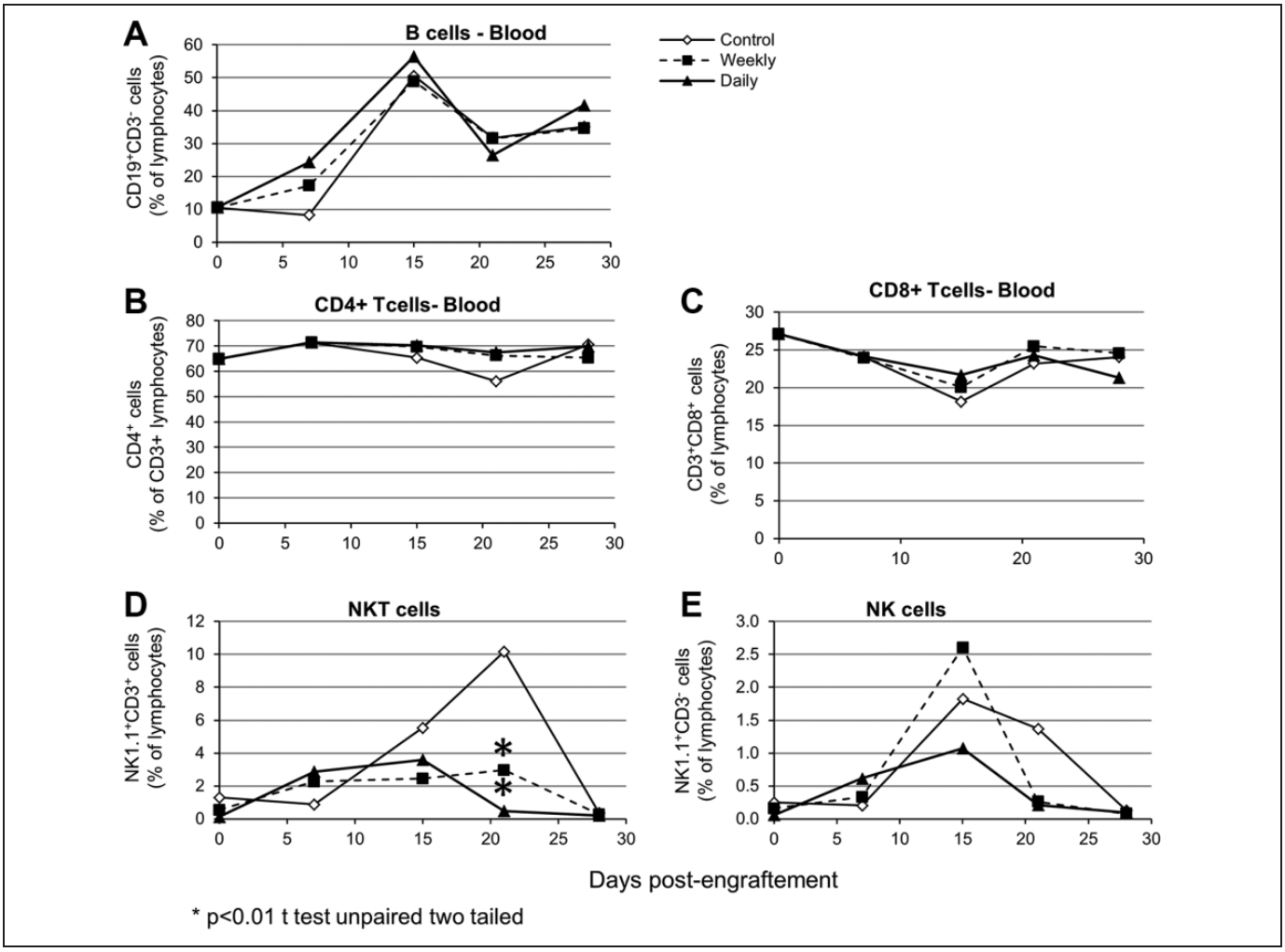

Figure 4. Lymphocytes subpopulations in blood samples throughout the study. Peripheral blood mononuclear cells were stained with fluorescent coupled anti-CD19, CD3, CD4, CD8, and NK1.1 antibodies. Signal was analyzed by flow cytometry and results were analyzed using FlowJo. Results are presented as percentage of lymphocytes, gated on size (FSC), and granularity (SSC). FSC indicates forward scatter; SSC, side scatter.

Cytokines often exhibit dual roles in cancer, depending on the expressing cells, the receiving cells, the microenvironment, or the combination of cytokines expressed, among others. With GM-CSF, IL7 was the most affected by exposure to the recording. These 2 cytokines are among the short list of cytokines in clinical trials for patients with advanced cancer.[17] Interleukin-7 promotes proliferation and maturation of lymphocytes and is being studied for its ability to enhance T-cell antitumor response in a variety of cancers.[18] In combination with IL15, it has been shown to decrease tumor volume and lung metastasis in murine melanoma and colon cancer models[19] and to induce antitumor immune cells in the 4T1 model.[20] Interestingly, we found that IL15 was also increased in the daily treated group, though this increase was not statistically significant.

The expression profiles of IL7 and IL15 were similar. Although the levels remained low in the control group, they were increased in both treatment groups as compared to the control group (Supplemental data 2). The levels of both IL7 and IL15 continued to increase at day 28. It has been suggested that the 2 cytokines can act together to increase infiltrating T cells.[21] In the present study, we did not see an increase in T cells in the blood nor did we see infiltrating T cells, except in necrotic areas within the tumor.

The other cytokines showing significant >2-fold changes were interleukin-12(p40) (IL12(p40)), IL10, IL1β, and IL6. Interleukin-12 is a dimeric protein with 2 subunits of 35 and 40 kb. Interleukin-12(p40) is shared with another cytokine, IL-23. Although IL12 is considered an antitumor cytokine, the p40 subunit may be detrimental to the activity of the whole protein by forming p40–p40 homodimers that act as competitive inhibitors of IL12.[22] A recent study showed that inhibition of IL12(p40) led to apoptosis in 4T1 cells.[23] Interleukin-12(p40) was decreased in the blood of mice treated weekly at day 28, indicating a potential antitumor effect of the recording. Interleukin-10 was also decreased in the spleen of treated mice at day 21. Interleukin-10 is usually considered

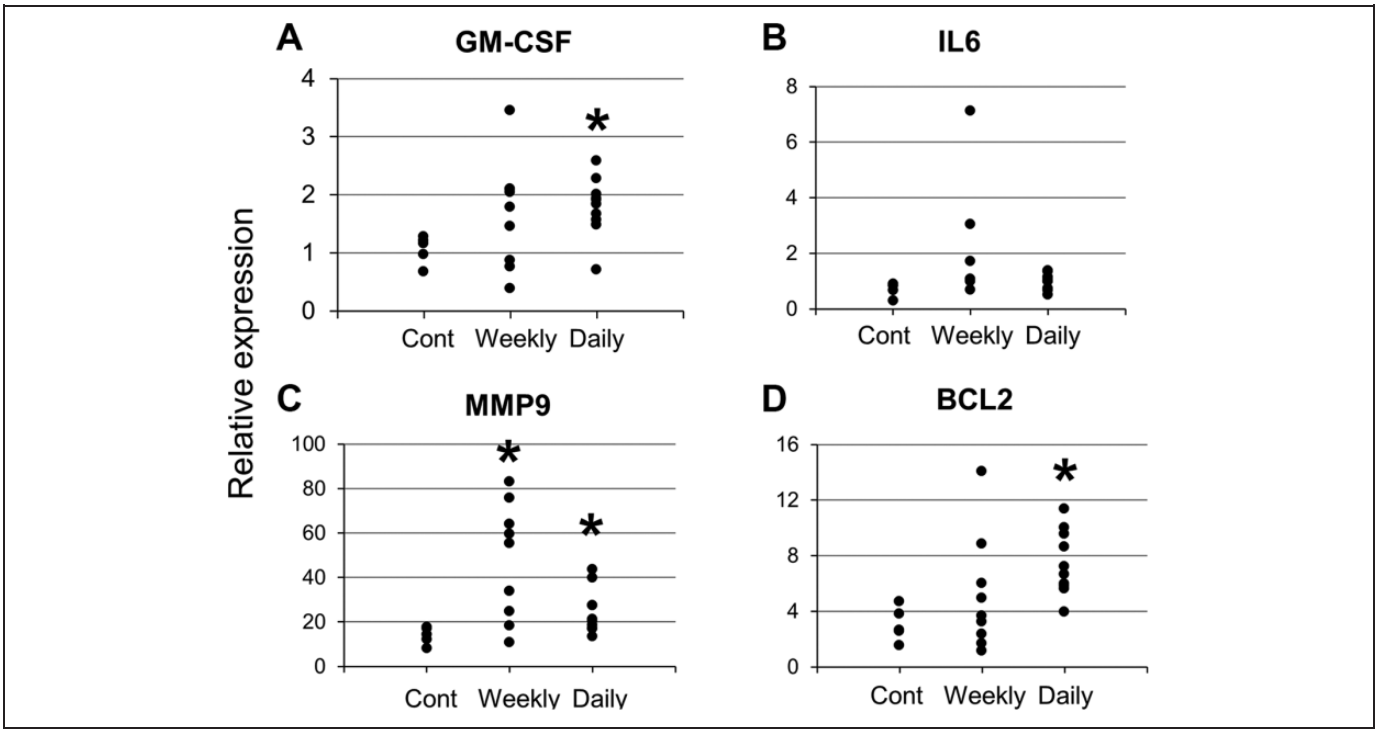

Figure 5. Expression of GM-CSF in the tumor. RNA was extracted and RT-qPCR was performed as previously described.[6] Each dot represents one animal and the relative expression was calculated with the $2^{-\Delta\Delta Ct}$ method. Significant differences when compared to the control group are shown with an asterisk (*; $P < .01$, unpaired, 2-tailed *t* test). GM-CSF indicates granulocyte–macrophage colony stimulating factor; qRT-PCR, quantitative real-time polymerase chain reaction.

Table 2. Fold-Change in Cytokine Levels.[a]

	Plasma Samples								Spleen Supernatant			
	D8		D14		D21		D28		D21		D28	
	Weekly	Daily	Weekly	Daily	Weekly	Daily	Weekly	Daily	Weekly	Daily	Weekly	Daily
GM-CSF			12.0	17.0	1.60							
			0.0577	**0.0128**	**0.0236**							
IL7					4.89							
					0.0097							
G-CSF												3.19
												0.0014
IL12(p40)							−3.07					
							0.0303					
IL10									−2.08	−1.72		
									0.0084	**0.0402**		
IL6										2.20		
										0.0328		
IL1B				5.80						1.88		2.02
				0.0577						**0.0353**		**0.0316**
IL15					2.30	2.08						
					0.0952	0.0673						

Abbreviations: D, day; GM-CSF, granulocyte–macrophage colony stimulating factor; IL, interleukin.

[a]Plasma samples (left) and supernatant from spleen cells (right) were analyzed to detect a panel of 25 cytokines using a milliplex-MAP assay. Data are presented as fold-change (upper value) and *P* value (*t* test, bottom value) compared to the control for each time point (D8, D14, D21, and D28). Only cytokines with significant changes >2-fold at 1 or more time points are displayed.

p values in bold are considered significant ($p < 0.05$).

Table 3. Expression of GM-CSF, IL6, BCL2, and MMP9 in Tumor Samples.[a]

	Weekly		Daily	
	Fold-Change	*P* Value	Fold-Change	*P* Value
GM-CSF	1.35	0.1856	1.66[b]	0.0089
IL6	2.24	0.2009	1.44	0.0857
BCL2	1.36	0.3054	2.51[b]	0.0017
MMP9	2.94[b]	0.0160	1.72[b]	0.0406

Abbreviations: BCL2, B-cell lymphoma 2; GM-CSF, granulocyte–macrophage colony stimulating factor; IL6, interleukin-6; MMP9, matrix metalloproteinase 9; qRT-PCR, quantitative real-time polymerase chain reaction.
[a]RNA was extracted and qRT-PCR was performed as previously described.[6] The table shows fold-changes and associated *P* values compared to the control in the weekly (gray) and daily (white) groups.
[b]Statistically significant fold-changes (Student *t* test, $P < .05$).

an immunosuppressive cytokine, and its inhibition could suggest a restoration of antitumor immune response. It is important to note that the decreases of IL12(p40) and IL10 were isolated and not observed at other time points.

Flow cytometry analysis indicated that there was no effect of the recording on B and T cells. Histological examination of the tumor confirmed this observation with the absence of CD4+ cells and the presence of CD8+ cells in necrotic areas in all groups (Supplemental data 1). We observed an increase in NK and NKT cells at days 15 and 21, suggesting a possible anticancer response. In the group of mice treated daily, this increase was lower but appeared earlier. Both NK and NKT cells, as part of innate immunity, are expected to appear early in the course of a disease. The earlier presence of NK and NKT cells in the daily group compared to the control group may indicate an earlier immune response to the tumor. A limitation to our interpretation of these results is that NK and NKT cells were present in very low proportions, and small variations (possibly due to variability between samples) can influence the final conclusions.

Previous work using hands-on techniques rather than the healing recording with the C3H/HeJ syngeneic model produced a reduction in tumor size after 4 to 6 weeks of daily hands-on treatment subsequent to engrafting.[24] In the present study, where we use the Balb/c/4T1 model, there was only a trend of tumors slowing down growth at day 28. The Balb/c/4T1 model might be less sensitive to this healing method.

There is evidence of a "loss of signal" when the recording is used. Previous in vitro work suggests weaker effects obtained from the recording alone when compared to hands-on methods.[6] Similarly, Balb/C/4T1 mice exposed to a hands-on method of healing showed a trend of smaller tumors in as early as 10 days. [11]

Whether this might be due to the limitations of recording technology or information outside the normal electromagnetic field spectrum remains unknown. Further investigations are necessary to determine the viability of this approach when compared to the traditional hands-on approach. Observations among experts in the field suggest that a live healer may be engaged in a dynamic feedback loop with the subject, whether either of them is aware of it or not. Perhaps, the use of physiological parameter (eg, heart rate variability) to modulate the strength or frequency of the recording could help bridge the gap between live healers and this recording.

Despite a possible loss of "signal" or information in the present method, this approach could still address the variability inherent to individuals practicing the healing method and scale up the delivery of the healing method.

In summary, our pilot study shows the following:

Exposure to the recording does not produce adverse effects. All animals in the treatment group were as "healthy" as in the control group, whether or not they were engrafted with tumor.

The recording did not induce a dramatic antitumor effect as measured by tumor volume within the time of the study (28 days), but at later time points, tumor volume in the control group was larger than in the treatment groups.

The recording induced a leukemoid reaction (increase in myeloid cells) in tumor-bearing mice.

The cytokine-level profile suggested an antitumor effect, but the recording may also have induced an IL6-mediated signal that could potentially promote tumor growth.

Our results suggest that the recording might have a biological effect on mice injected with cancer cells, but it will be important to better characterize this effect by reproducing this experimental design with longer predefined end points followed by a refinement of dose, frequency, and duration of treatment.

Acknowledgments

The authors thank David Dominik for his generous support and Mark Dooner for his assistance in using equipment.

Declaration of Conflicting Interests

The author(s) declared the following potential conflicts of interest with respect to the research, authorship, and/or publication of this article: WB is the inventor of the Bengston Healing Method and author of works describing the method.

Funding

The author(s) disclosed receipt of the following financial support for the research, authorship, and/or publication of this article: Immunostaining reported in this publication was supported by the Molecular Pathology Core of the COBRE Center for Cancer Research Development, funded by the National Institute of General Medical Sciences (NIGMS) of the National Institutes of Health under Award Number P30GM110759. The previous segments of this project were supported by the NIGMS under P20GM103421 and National Center for Research Resources (NCRR) under P20RR017695. This research was funded through generous donations from The Emerald Gate Charitable Trust.

ORCID iD

Sarah Beseme https://orcid.org/0000-0002-9318-1239

Supplemental Material

Supplemental material for this article is available online.

References

1. Yun H, Sun L, Mao JJ. Growth of integrative medicine at leading cancer centers between 2009 and 2016: a systematic analysis of NCI-designated comprehensive cancer center websites. *J Natl Cancer Inst Monographs*. 2017;2017(52). doi:10.1093/jncimonographs/lgx004.
2. Garland SN, Valentine D, Desai K, et al. Complementary and alternative medicine use and benefit finding among cancer patients. *J Altern Complement Med*. 2013;19(11):876-881. doi:10.1089/acm.2012.0964.
3. Rao A, Hickman LD, Sibbritt D, Newton PJ, Phillips JL. Is energy healing an effective non-pharmacological therapy for improving symptom management of chronic illnesses? A systematic review. *Complement Ther Clin Pract*. 2016;25:26-41. doi:10.1016/j.ctcp.2016.07.003
4. Bengston WF. Commentary: a method used to train skeptical volunteers to heal in an experimental setting. *J Altern Complement Med*. 2007;13(3):329-331. doi:10.1089/acm.2007.6403
5. Bengston W. Hands-On Healing: A Training Course on the Energy Cure. Sounds True. 2010
6. Beseme S, Bengston W, Radin D, Turner M, McMichael J. Transcriptional changes in cancer cells induced by exposure to a healing method. *Dose Response*. 2018;16(3). doi:10.1177/1559325818782843
7. DuPré SA, Redelman D, Hunter KW. The mouse mammary carcinoma 4T1: characterization of the cellular landscape of primary tumours and metastatic tumour foci. *Int J Exp Pathol*. 2007;88(5):351-360. doi:10.1111/j.1365-2613.2007.00539.x.
8. Sevmis M, Yoyen-Ermis D, Aydin C, et al. Splenectomy-induced leukocytosis promotes intratumoral accumulation of myeloid-derived suppressor cells, angiogenesis and metastasis. *Immunol Invest*. 2017;46(7):663-676. doi:10.1080/08820139.2017.1360339.
9. Kothari P, Pestana R, Mesraoua R, et al. IL-6-mediated induction of matrix metalloproteinase-9 is modulated by JAK-dependent IL-10 expression in macrophages. *J Immunol*. 2014;192(1):349-357. doi:10.4049/jimmunol.1301906.
10. Fisher DT, Appenheimer MM, Evans SS. The two faces of IL-6 in the tumor microenvironment. *Semin Immunol*. 2014;26(1):38-47. doi:10.1016/j.smim.2014.01.008.
11. Running A, Greenwood M, Hildreth L, Schmidt J. Bioenergy and breast cancer: a report on tumor growth and metastasis. *Evid Based Complement Alternat Med*. 2016;2016. doi:10.1155/2016/2503267.
12. Dolcetti L, Peranzoni E, Ugel S, et al. Hierarchy of immunosuppressive strength among myeloid-derived suppressor cell subsets is determined by GM-CSF. *Eur J Immunol*. 2010;40(1):22-35. doi:10.1002/eji.200939903.
13. Morales JK, Kmieciak M, Knutson KL, Bear HD, Manjili MH. GM-CSF is one of the main breast tumor-derived soluble factors involved in the differentiation of CD11b-Gr1− bone marrow progenitor cells into myeloid-derived suppressor cells. *Breast Cancer Res Treat*. 2010;123(1):39-49. doi:10.1007/s10549-009-0622-8.
14. Mach N, Gillessen S, Wilson SB, Sheehan C, Mihm M, Dranoff G. Differences in dendritic cells stimulated in vivo by tumors engineered to secrete granulocyte-macrophage colony-stimulating factor or Flt3-ligand. *Cancer Res*. 2000;60(12):3239-3246.
15. Gillessen S, Naumov YN, Nieuwenhuis EES, et al. CD1d-restricted T cells regulate dendritic cell function and antitumor immunity in a granulocyte–macrophage colony-stimulating factor-dependent fashion. *Proc Natl Acad Sci U S A*. 2003;100(15):8874-8879. doi:10.1073/pnas.1033098100.
16. Chiang CS, Fu SY, Wang SC, et al. Irradiation promotes an M2 macrophage phenotype in tumor hypoxia. *Front Oncol*. 2012;2:89. doi:10.3389/fonc.2012.00089.
17. Conlon KC, Miljkovic MD, Waldmann TA. Cytokines in the treatment of cancer. *J Interferon Cytokine Res*. 2019;39(1):6-21. doi:10.1089/jir.2018.0019.
18. Lin J, Zhu Z, Xiao H, et al. The role of IL-7 in immunity and cancer. *Anticancer Res*. 2017;37(3):963-967. doi:10.21873/anticanres.11405.
19. Song Y, Liu Y, Hu R, Su M, Rood D, Lai L. In vivo antitumor activity of a recombinant IL7/IL15 hybrid cytokine in mice. *Mol Cancer Ther*. 2016;15(10):2413-2421. doi:10.1158/1535-7163.MCT-16-0111.
20. Cha E, Graham L, Manjili MH, Bear HD. IL-7 + IL-15 are superior to IL-2 for the ex vivo expansion of 4T1 mammary carcinoma-specific T cells with greater efficacy against tumors in vivo. *Breast Cancer Res Treat*. 2010;122(2):359-369. doi:10.1007/s10549-009-0573-0.
21. Xu X, Sun Q, Mei Y, Liu Y, Zhao L. Newcastle disease virus co-expressing interleukin 7 and interleukin 15 modified tumor cells as a vaccine for cancer immunotherapy. *Cancer Sci*. 2018;109(2):279-288. doi:10.1111/cas.13468.
22. Ling P, Gately MK, Gubler U, et al. Human IL-12 p40 homodimer binds to the IL-12 receptor but does not mediate biologic activity. *J Immunol*. 1995;154(1):116-127.
23. Kundu M, Roy A, Pahan K. Selective neutralization of IL-12 p40 monomer induces death in prostate cancer cells via IL-12–IFN-γ. *Proc Natl Acad Sci U S A*. 2017;114(43):11482-11487. doi:10.1073/pnas.1705536114.
24. Bengston WF, Krinsley D. The effect of the "laying on of hands" on transplanted breast cancer in mice. *J Sci Explor*. 2000;14(3):353-364.